

Evaluation of Current Controllers for Distributed Power Generation Systems

Adrian Timbus, *Student Member, IEEE*, Marco Liserre, *Senior Member, IEEE*,
Remus Teodorescu, *Senior Member, IEEE*, Pedro Rodriguez, *Member, IEEE*, and Frede Blaabjerg, *Fellow, IEEE*

Abstract—This paper discusses the evaluation of different current controllers employed for grid-connected distributed power generation systems having variable input power, such as wind turbines and photovoltaic systems. The focus is mainly set on linear controllers such as proportional–integral, proportional–resonant, and deadbeat (DB) controllers. Additionally, an improved DB controller robust against grid impedance variation is also presented. Since the paper discusses the implementation of these controllers for grid-connected applications, their evaluation is made in three operating conditions. First, in steady-state conditions, the contribution of controllers to the total harmonic distortion of the grid current is pursued. Further on, the behavior of controllers in the case of transient conditions like input power variations and grid voltage faults is also examined. Experimental results in each case are presented in order to evaluate the performance of the controllers.

Index Terms—Current controllers, current harmonic distortion, distributed power generation systems (DPGSs), grid faults, input power variations.

I. INTRODUCTION

TODAY, distributed power generation systems (DPGSs) based on renewable energies are no longer regarded as one of the engineering challenges but as a potential player that can have a major contribution to the total energy production worldwide. In the last decade, exponential growth of both wind turbines (WTs) and photovoltaic (PV) power generation systems is registered [1], [2].

However, due to the stochastic behavior of the input power for both WT and PV systems, their controllability is an important issue to be considered when these systems are connected to the utility network [3]. Due to the large penetration of renewable systems in some of the European countries, more stringent interconnection demands are requested by the power system operators. The power quality and robustness to the grid voltage and frequency variations are two of the main points demanded in the latest issues of grid codes for WTs in Germany, Denmark, and

Manuscript received June 1, 2007; revised January 10, 2008. First published March 16, 2009; current version published April 8, 2009. Recommended for publication by Associate Editor M. G. Simoes.

A. Timbus is with Corporate Research, ABB Switzerland Ltd., Baden-Daettwil CH-5405, Switzerland (e-mail: adrian.timbus@ch.abb.com).

M. Liserre is with the Department of Electrotechnical and Electronic Engineering, Polytechnic of Bari, Bari 70125, Italy (e-mail: liserre@iee.edu).

R. Teodorescu and F. Blaabjerg are with the Institute of Energy Technology, Aalborg University, Aalborg DK-9220, Denmark (e-mail: ret@iet.aau.dk; fbl@iet.aau.dk).

P. Rodriguez is with the Department of Electrotechnical and Electronic Engineering, Technical University of Catalonia, Terrassa-Barcelona 08222, Spain (e-mail: prodiguez@ee.upc.edu).

Color versions of one or more of the figures in this paper are available online at <http://ieeexplore.ieee.org>.

Digital Object Identifier 10.1109/TPEL.2009.2012527

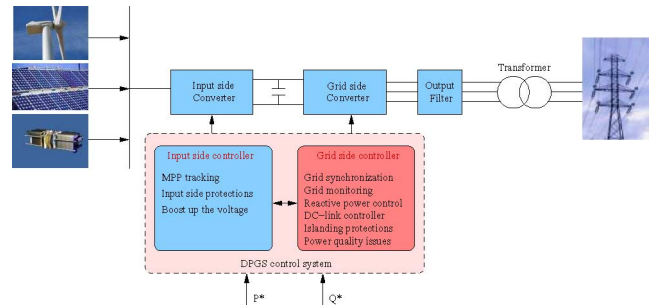


Fig. 1. General structure of a renewable energy DPGS and its main control features.

Spain [4], [5]. Consequently, there is a large interest in studying the control capabilities of distributed systems in situations of grid fault conditions.

This paper discusses the control issues of the DPGS in order to fulfill the grid demands regarding power quality and grid faults ride-through. Since the demands are more stringent in the WT case, focus is set on these systems rather than PV systems.

First, a general structure of a DPGS is described, highlighting some possible control tasks. Second, the grid converter control is analyzed in detail, and possible control loops and considerations in case of grid faults are given. Further on, the considered controllers are investigated and evaluated in terms of power quality, input power variations, and low-voltage grid ride-through. Finally, experimental results are presented to validate the evaluation of the controllers discussed in this paper.

II. DPGS STRUCTURE AND CONTROL

A. DPGS Structure

A general structure of a distributed generation system is depicted in Fig. 1. Depending on the input power nature, i.e., wind, sun, and hydrogen, numerous hardware configurations are possible [3], [6]. In this paper, a system having a full-size back-to-back converter configuration is considered. In this situation, there is an *input side controller* that controls the input side converter and a *grid side controller* that takes care of the DPGS interaction with the utility grid.

B. DPGS Control

One of the main tasks of input side controller is to extract the maximum power from the input power source and to transmit this to the grid side controller. In the case of grid failure, this controller should also protect the input power source. In the case of WT systems, the input side controller has different tasks,

TABLE I
DISTORTION LIMITS FOR DPGS SYSTEMS WHEN INTERCONNECTING
THE UTILITY NETWORK

Odd harmonics	Distortion limit
$3^{rd} - 9^{th}$	< 4.0 %
$11^{th} - 15^{th}$	< 2.0 %
$17^{th} - 21^{st}$	< 1.5 %
$23^{rd} - 33^{rd}$	< 0.6 %

depending on the generator type used. On the other hand, the grid side controller normally regulates the dc-link voltage in order to maintain the power balance and takes care about the quality of the generated power by controlling the output current. Synchronization with the grid voltage and grid (voltage and frequency) monitoring is also an important task of this controller. Since in the considered topology, the output power is completely decoupled from the input power by a dc link, the grid side converter is mainly responsible for the fault tolerance of such a power generation system.

III. GRID DEMANDS

As mentioned previously, due to the exponential increase of WT and PV systems connected to the utility network, more restrictive demands imposed by the transmission system operators (TSOs) are issued in order to maintain a proper functionality of the power system.

A. Power Quality Issues

For both WT and PV systems, the maximum limit for the total harmonic distortion (THD) of the output current is set to 5% according to the IEEE Standard 15471 [7]. Similar limitations are recommended for PV systems in an International Electrotechnical Commission (IEC) standard [8]. As regards WT systems, IEC standards recommend a pollution smaller than 6%–8% depending on the type of network to which the turbines are connected [9]–[11]. In order to comply with these requirements, the current controller should have a very good harmonic rejection, especially for low-order harmonics that normally have a higher content in the power system.

Table I shows the maximum allowed distortion limits for the first 33 current harmonics, according to [7].

B. Voltage Variation Issues

In addition to the power quality demands, the TSOs also require the capability of the generation systems to ride-through short grid voltage variations. Considering the installation of a WT into the Danish utility grid, the voltage variations and corresponding ride-through times, published in [5] and depicted in Fig. 2, should be fulfilled. As it may be noted, the WT should have a ride-through capability of 0.1 s when the grid voltage amplitude register a dip down to 25% of its nominal value. On the other hand, the generation system should also ride-through for a voltage being 120% of its nominal value. As a consequence, the grid side controller should be prepared for such situations

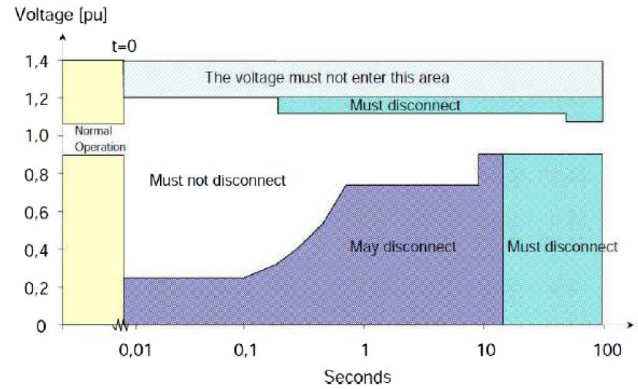


Fig. 2. Illustration of the grid voltage variations and the disconnection boundaries for WTs connected to the Danish power system.

in order to avoid the disconnection of the generation unit and comply with the demands.

Depending on the number of phases that register such a dip, the power system can remain balanced if all three phases are dropping with the same amplitude, or it can become unbalanced if one or two phases experience such a fault [12].

In addition to the power quality and voltage variations, there are many other requirements stated in the grid codes for WT systems, i.e., grid frequency variations, reactive power control, etc., but their discussion here is less relevant for the purpose of this paper.

IV. CONTROL STRUCTURES FOR GRID CONVERTER

In the following, a few control structures for the grid converter are discussed. The implementation of the control strategy for a distributed generation system can be done in different reference frames such as synchronous rotating (dq), stationary ($\alpha\beta$), or reference (abc) frame. The focus is set on different controller types and their implementation in different reference frames.

A. The dq Control

The dq control structure is using the $abc \rightarrow dq$ transformation module to transform the control variables from their natural frame abc to a frame that synchronously rotates with the frequency of the grid voltage. As a consequence, the control variables are becoming dc signals. Specific to this control structure is the necessity of information about the phase angle of utility voltage in order to perform the transformation. Normally, proportional–integral (PI) controllers are associated with this control structure. A typical transfer function of a PI controller is given by

$$G_{PI}(s) = K_p + \frac{K_i}{s} \quad (1)$$

where K_p is the proportional and K_i is the integral gain of the controller. The structure of dq control involving cross coupling and feedforward of the grid voltages is depicted in Fig. 3. Since grid voltage feedforward is used in this control structure, the dynamics of the control is expected to be high during grid voltage fluctuations. Every deviation of the grid voltage amplitude will

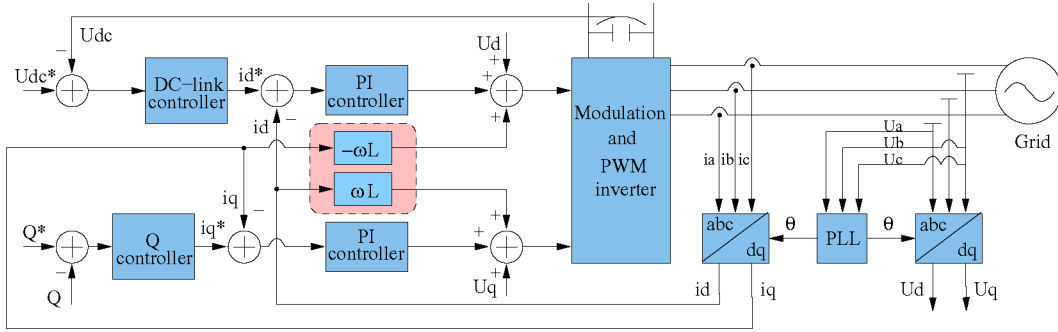


Fig. 3. General structure for synchronous rotating frame control using cross-coupling and voltage feedforward terms.

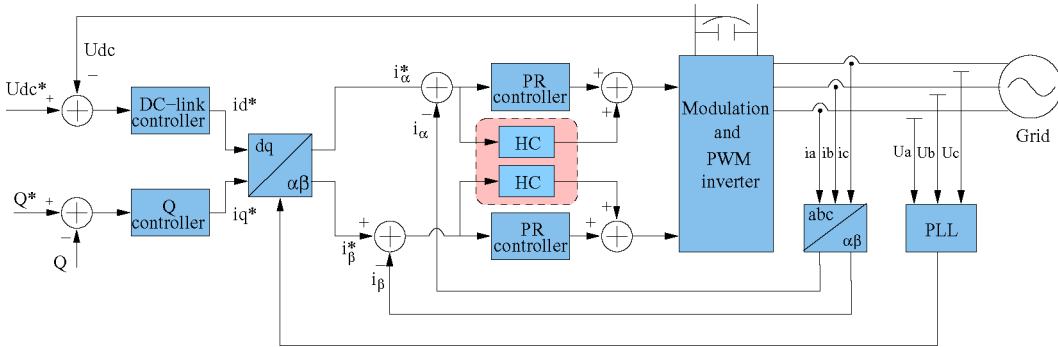


Fig. 4. General structure for stationary reference frame control strategy using resonant controllers and harmonic compensators.

be reflected into the d - and q -axis component of the voltage, leading to a fast response of the control system.

B. Stationary Frame Control

Since in the case of stationary reference frame control, the control variables, e.g., grid currents, are time-varying waveforms, PI controllers encounter difficulties in removing the steady-state error. As a consequence, another type of controller should be used in this situation.

The proportional-resonant (PR) controller [13]–[16] gained a large popularity in the last decade due to its capability of eliminating the steady-state error when regulating sinusoidal signals, as is the case of $\alpha\beta$ or abc control structures. Moreover, easy implementation of a harmonic compensator for low-order harmonics without influencing the controller dynamics makes this controller well suited for grid-tied systems [17]. The transfer function of resonant controller is defined as

$$G_{PR}(s) = K_p + K_i \frac{s}{s^2 + \omega^2}. \quad (2)$$

Because this controller acts on a very narrow band around its resonant frequency ω , the implementation of harmonic compensator for low-order harmonics is possible without influencing at all the behavior of the current controller [17]. The transfer function of the harmonic compensator is given by

$$G_{HC}(s) = \sum_{h=3,5,7} K_{ih} \frac{s}{s^2 + (\omega h)^2} \quad (3)$$

where h denotes the harmonic order that the compensator is implemented for. A general structure of a stationary reference

frame control using resonant controllers and harmonics compensators is illustrated in Fig. 4.

Note that both (2) and (3) use information about the resonant frequency at which the controller operates. For the best performance of the resonant controller, this frequency has to be identical to the grid frequency. Hence, it should be remarked that an adaptive adjustment of the controller frequency is necessary if grid frequency variations are registered in the utility network, as reported in [18].

C. The abc Frame Control

Historically, the control structure implemented in abc frame is one of the first structures used for pulsewidth modulation (PWM) driven converters [19], [20]. Usually, implementation of nonlinear controllers such as hysteresis controller has been used. The main disadvantage of these controllers was the necessity of high sampling rate in order to obtain high performance. Nowadays, due to the fast development of digital devices such as microcontrollers (MCs) and DSPs, implementation of nonlinear controllers for grid-tied applications becomes very actual.

In case of abc control, it is worthwhile to remark that in the situation of an isolated neutral transformer, as is the case of DPGS using a Δy transformer as grid interface, only two of the grid currents can be independently controlled, the third one being the negative sum of the other two, according to Kirchhoff current law. Hence, the implementation of only two controllers is necessary in this situation [21]. The following paragraphs describe the implementation of PI, PR, and deadbeat (DB) controllers in stationary abc frame.

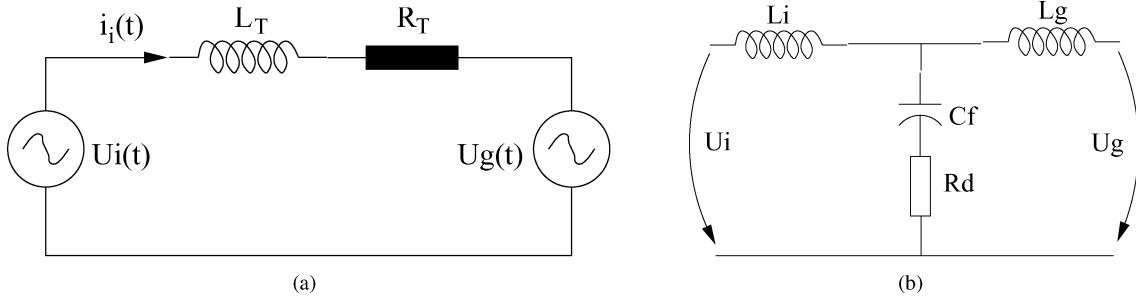


Fig. 5. (a) Representation of single-phase circuit used to derive the DB controller equation, where $L_T = L_i + L_g$ and $R_T = R_i + R_g$. (b) Single-phase representation of the LCL filter used to calculate the gains of the controllers.

1) *PI Controller*: The portability of the PI controller to another reference frame like the stationary frame has been derived in [21] using transformation modules between the frames. Moreover, in [22], the equivalent of PI controller in abc frame has been derived, as shown (4), at the bottom of this page. Note in this case that the complexity of the controller matrix is due to the off-diagonal terms due to the cross-coupling terms between the phases.

2) *Resonant Controller*: Since the PR controller is already defined in stationary reference frame, its portability to a natural frame is a straight solution. The controller matrix in this case is given by (5).

$$G_{\text{PR}}^{(abc)}(s) = \begin{bmatrix} K_p + \frac{K_i s}{s^2 + \omega_0^2} & 0 & 0 \\ 0 & K_p + \frac{K_i s}{s^2 + \omega_0^2} & 0 \\ 0 & 0 & K_p + \frac{K_i s}{s^2 + \omega_0^2} \end{bmatrix}. \quad (5)$$

As there is no cross-coupling terms to account for phases interaction in this case, (5) cannot be used when the neutral of the transformer is isolated, in this situation only two controllers being necessary, as described in [21].

3) *DB Controller*: Belonging to the family of predictive controllers, DB controller is widely employed for sinusoidal current regulation of different applications due to its high dynamic response [23]–[30]. In order to achieve best reference tracking, the working principle of DB controller is to calculate the derivative of the controlled variable (grid current in this case) in order to predict the effect of the control action. This controller has theoretically a very high bandwidth, and hence, tracking of sinusoidal signals is very good. However, if PWM and saturation

of the control action are considered, the DB controller exhibits slower response.

The equation of predictive DB controller can be derived using Kirchhoff's law on the single-phase circuit shown in Fig. 5(a). In this case, the equation for the current through the inverter i_i (controlled current) can be expressed as

$$\frac{di_i(t)}{dt} = -\frac{R_T}{L_T}i_i(t) + \frac{1}{L_T}(U_i(t) - U_g(t)) \quad (6)$$

where L_T is the total inductance and R_T is the total resistance upstream of the grid converter, and $U_i(t)$ and $U_g(t)$ are the inverter and grid voltages, respectively. The discretized form of (6) is given by

$$i_i((k+1)T_s) = e^{-(R_T/L_T)T_s}i_i(kT_s) - \frac{1}{R_T}(e^{-(R_T/L_T)T_s} - 1)(U_i(kT_s) - U_g(kT_s)). \quad (7)$$

Solving (7), the controller equation can be derived as

$$G_{\text{DB}}^{(abc)} = \left(\frac{1}{b}\right) \left(\frac{1 - az^{-1}}{1 - z^{-1}}\right) \quad (8)$$

where a and b are denoted as

$$a = e^{-(R_T/L_T)T_s}, \quad b = -\frac{1}{R_T}(e^{-(R_T/L_T)T_s} - 1). \quad (9)$$

Finally, the controller algorithm can be implemented as

$$U_i((k+1)T_s) = U_i((k-1)T_s) + \frac{1}{b}\Delta i(kT_s) - \frac{a}{b}\Delta i((k-1)T_s) + U_g((k+1)T_s) - U_g((k-1)T_s). \quad (10)$$

Again, because the controller equation in this case has been derived considering a single-phase circuit, implementation of only two such controllers is necessary in the situation of an

$$G_{\text{PI}}^{(abc)}(s) = \frac{2}{3} \begin{bmatrix} K_p + \frac{K_i s}{s^2 + \omega_0^2} & -\frac{K_p}{2} - \frac{K_i s + \sqrt{3}K_i\omega_0}{2(s^2 + \omega_0^2)} & -\frac{K_p}{2} - \frac{K_i s - \sqrt{3}K_i\omega_0}{2(s^2 + \omega_0^2)} \\ -\frac{K_p}{2} - \frac{K_i s - \sqrt{3}K_i\omega_0}{2(s^2 + \omega_0^2)} & K_p + \frac{K_i s}{s^2 + \omega_0^2} & -\frac{K_p}{2} - \frac{K_i s + \sqrt{3}K_i\omega_0}{2(s^2 + \omega_0^2)} \\ -\frac{K_p}{2} - \frac{K_i s + \sqrt{3}K_i\omega_0}{2(s^2 + \omega_0^2)} & -\frac{K_p}{2} - \frac{K_i s - \sqrt{3}K_i\omega_0}{2(s^2 + \omega_0^2)} & K_p + \frac{K_i s}{s^2 + \omega_0^2} \end{bmatrix} \quad (4)$$

isolated neutral transformer, the third grid current being given by the Kirchhoff's law.

Since DB controller controls the current such that this reaches its reference at the end of next switching period, the controller is introducing one sample time delay. In order to compensate for this delay and the plant nonlinearities, an observer can be introduced in the structure of the controller [27]. Moreover, a fuzzy logic controller tuned on the basis of DB theory and then modified online in order to take into account the unmodeled nonlinearities is also possible [31].

V. DESIGN OF LINEAR CONTROLLERS

A. Model of the Plant

The plant considered in this application is the *LCL* filter attached to the power converter. In this case, only an *LC* filter is physically implemented, while the second *L* is the inductance of the transformer, as shown in Fig. 9. The filter transfer function has been derived using its single-phase electrical diagram illustrated in Fig. 5(b).

The relation for the currents flowing through the filter is given by

$$i_i - i_c - i_g = 0 \quad (11)$$

while the voltages can be described by

$$U_i = i_i L_i s + U_c \quad (12a)$$

$$U_g = -i_g L_g s + U_c \quad (12b)$$

$$U_c = i_c \left(\frac{1}{C_f s} + R_d \right). \quad (12c)$$

Deriving the current values yields

$$i_i = \frac{1}{L_i s} (U_i - U_c), \quad i_g = \frac{1}{L_g s} (U_c - U_g) \quad (13)$$

where s denotes the Laplace operator. Rewriting in terms of impedances, the voltages can be derived as

$$\begin{aligned} U_i &= z_{11} i_i + z_{12} i_g \\ U_g &= z_{21} i_i + z_{22} i_g \end{aligned} \quad (14)$$

where

$$\begin{aligned} z_{11} &= L_i s + \frac{1}{C_f s} + R_d, \quad z_{12} = - \left(\frac{1}{C_f s} + R_d \right) \\ z_{22} &= - \left(L_g s + \frac{1}{C_f s} + R_d \right), \quad z_{21} = \frac{1}{C_f s} + R_d. \end{aligned} \quad (15)$$

Developing the relations for grid current and voltage, the transfer function of the plant is finally obtained as

$$\begin{aligned} H(s) &= \frac{i_g}{U_i} = \frac{z_{21}}{z_{12} z_{21} - z_{11} z_{22}} \\ &= \frac{R_d C_f s + 1}{L_i L_g C_f s^3 + R_d C_f (L_i + L_g) s^2 + (L_i + L_g) s} \end{aligned} \quad (16)$$

where L_i and C_f are the filter inductance and capacitance, respectively, L_g is the transformer inductance, and R_d is the damping resistance.

TABLE II
LCL OUTPUT FILTER PARAMETERS

Inverter side impedance	Capacitance	Grid side impedance
$L_i = 10 \text{ mH}$	$C_f = 0.7 \mu\text{F}$	$L_g = 2 \text{ mH}$
$R_i = 0.4 \Omega$	$R_d = 0 \Omega$	$R_g = 0.6 \Omega$

The *LCL* filter parameters are listed in Table II. As mentioned previously, the grid side parameters L_g and R_g are representing the transformer.

B. Resonant Controller Design

The PR controller is tuned based on the root locus theory. Using the controller transfer function given in (2) and the plant transfer function from (16), the closed-loop transfer function is derived in discrete form like

$$\text{CL}(z) = \frac{\text{PR}(z)H(z)}{1 + \text{PR}(z)H(z)} \quad (17)$$

where $\text{PR}(z)$ and $H(z)$ are the discrete forms of (2) and (16), respectively, derived using *c2d* facility in MATLAB. The root loci of the closed-loop system shown in Fig. 6(a) are used to tune the resonant controller. The controller has been designed for having a damping of $\zeta = 1/\sqrt{2}$, and in this case, the proportional gain of the controller has been obtained as $K_p = 30$. The value for the integral gain of the controllers K_i has been obtained using Bode plot of the open-loop system shown in Fig. 6(b), where the value of $K_i = 6000$ has been selected for implementation, which provides a very high gain at the resonant frequency of the controller (50 Hz in this case), thus having a good steady-state error rejection.

C. PI Controller Design

Because the values of the controller gains are not changing when the controller is transformed in different reference frames [21], the same values for K_p and K_i are used for the PI controllers as well (in both *dq* and *abc* implementations).

D. DB Controller Design

Since the DB controller is developed on the basis of filter and grid model, it is sensitive to model and parameter mismatch. Several modalities to improve the robustness to parameters discordance are presented in [27] and [32]–[34]. In addition, the presence of filter capacitance make the closed-loop system to become unstable. As illustrated in Fig. 7(a), in situation when *LCL* filter is used, high-frequency poles are placed near the instability border, and hence, any disturbance can take the system out of stability. In this paper, a novel solution to improve the robustness of the DB controller in the situation of plant parameters change has been developed. The proposed method increases artificially the gain b of the controller in respect to its initial value calculated by (9). As Fig. 7(a) illustrates, by increasing b , the damping in the system is increased, and additionally, high-frequency poles are moving inside the unity circle, ensuring the system stability. By doing this, the behavior of DB controller using an *LCL* filter is similar with that when only *L* filter is used, as shown in Fig. 7(b) and (c). In addition, this method has been tested in

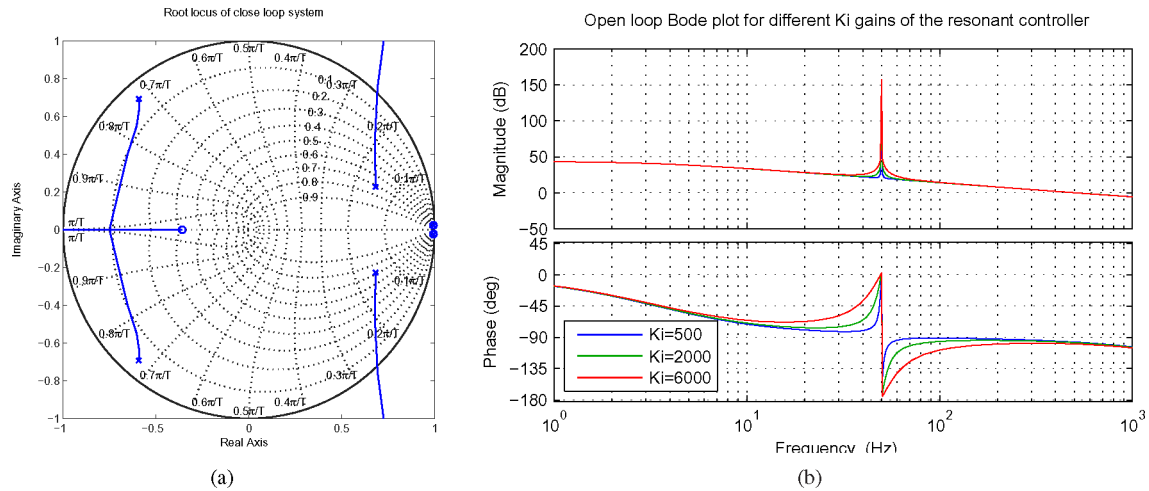


Fig. 6. Tuning methods for resonant controller. (a) Root loci of the closed-loop system (17). (b) Bode plot of the open loop in the case of different values for the integral gain K_i .

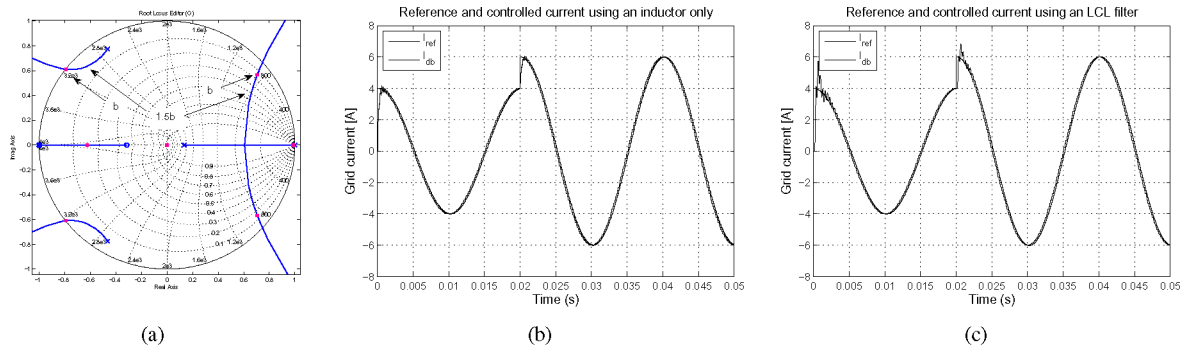


Fig. 7. Design criteria and performance of robust DB controller. (a) Pole zero map of the controller. (b) Controller response to a step disturbance in case only L filter is used. (c) Controller response in case LCL filter is used and the gain b is artificially increased to maintain stability.

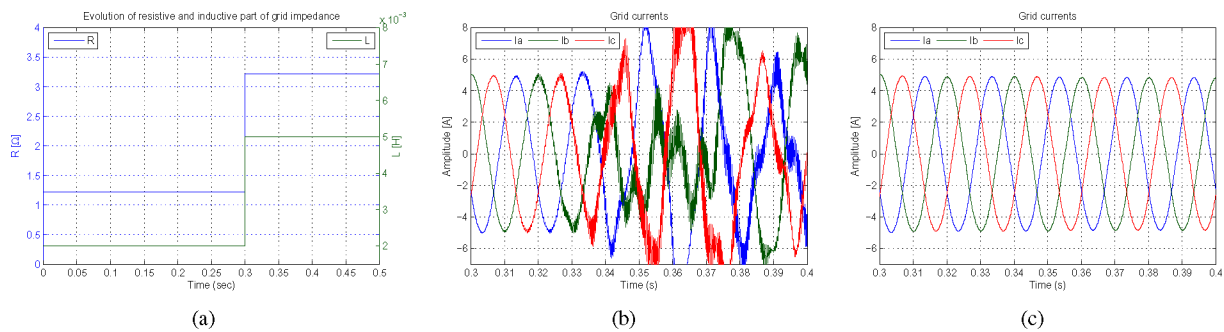


Fig. 8. Performance of robust DB controller in situation of grid impedance variation. (a) Operating conditions. (b) Conventional DB controller performance. (c) Behavior of robust DB controller during impedance variation.

many simulation models having different levels of parameters mismatch. In all cases, an increase of gain b with about 50% of its normal value initially calculated using (9) leads to a robust DB controller that is able to regulate the current even though the grid parameters have large variations from their initial values. Depending on the values of LCL filter components, the increase of b could be less or more than 50% of its original value. In order to assess the right value of b for any operation conditions

and different power ratings, the pole-zero map of each particular system should be analyzed.

Fig. 8(a) illustrates the situation when grid impedances (both resistive and inductive parts) are registering large variations. In such case, the conventional DB controller having the gain b calculated by (9) encounters difficulties to control the current after the impedance value has changed, as depicted in Fig. 8(b). On the other hand, artificial increase of gain b leads to a robust

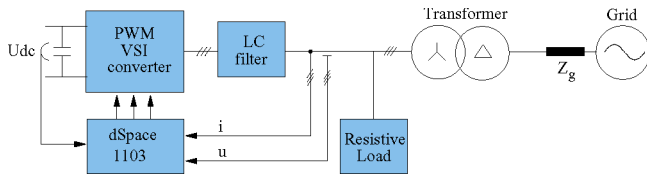


Fig. 9. Schematic of the laboratory setup connected to a grid simulator through a $\Delta\gamma$ transformer and having a resistive load.

DB controller able to operate over a large band of impedance values, as shown in Fig. 8(c).

VI. LABORATORY IMPLEMENTATION

To be able to evaluate the behavior of the different control structures and controllers, an experimental setup having the schematic as depicted in Fig. 9 has been implemented in laboratory. The filter parameters are as described in Section V-A (matching exactly the ones set in simulation) and the power converter is a Danfoss VLT 5000 series rated for 400 V and 5 A. Since the grid simulator cannot accept power, a local load is connected in the circuit. The load is pure resistive and is sized in the way that the current through the load is the sum of the converter current and the grid current. The grid currents and voltages as well as the dc-link voltage are sampled and used in the control structures described in Section IV and illustrated in Fig. 9.

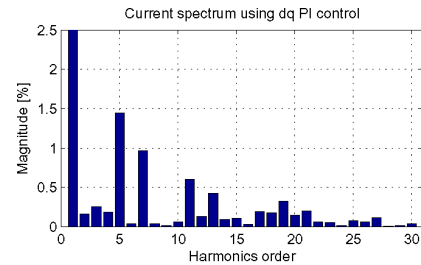
The controllers and the control structures are implemented using a dSpace 1103 board having a 333-MHz power PC (PPC) processor. All control structures are implemented at a sampling and switching frequency of 13 kHz. In this paper, experimental results for four control structures are presented, i.e., PI controllers implemented in dq frame [see (1)], PR implemented in $\alpha\beta$ stationary frame [see (2)], the equivalent of PI in abc frame [see (4)], and DB controller implemented in abc frame [see (8)]. For a fair evaluation of the controllers, only the current loop is considered; hence, the influence of the dc-link controller or any other outer loop control is eliminated.

VII. EXPERIMENTAL RESULTS

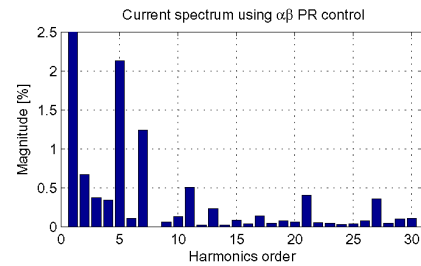
The evaluation of the control structures and controllers is made in two situations, i.e., steady-state and transient operations. In a steady-state situation, the quality of the controlled current is discussed, while in the transient operation conditions, the controller response to a step increase of the current reference and to a single-phase grid fault is studied.

A. Steady-State Operation

The pollution rate of the controllers is determined in the situation of ideal grid conditions. The grid simulator is programmed to provide a perfect sinusoidal output voltage containing no harmonics; hence, the harmonics of the grid current are due to the current controller and system nonlinearity. In all the cases, the THD of the current is measured using a three-phase Voltech PM3000 power meter.



(a)



(b)

Fig. 10. Harmonic spectrum of the grid current in the case of (a) dq PI control and (b) stationary control using PR controller.

1) *Synchronous Rotating Frame Control*: The THD of the grid current in the case of dq control employing PI controllers for current regulation is shown in Fig. 10(a). The first 30 harmonics are shown, and as can be observed, the fifth and seventh harmonics are having the larger contribution to the grid current THD, which in this case was measured to be 1.77%. It is worth noting that no filtering has been used for the voltage feedforward terms U_d and U_q that are provided by the transformation module $abc \rightarrow dq$, as illustrated in Fig. 3.

2) *Stationary Frame Control*: As mentioned previously, in the case of stationary frame control, the resonant controller is used for current regulation. In order to have a fair comparison between the structures and controllers, the harmonic compensator has not been considered here. As a consequence, a larger magnitude for the fifth and seventh harmonics is registered in this case, as can be observed in Fig. 10(b). The THD value of the delivered current in this situation is 2.6%.

3) *Natural Frame Control*: In the case of natural frame control, two controller types are implemented, i.e., equivalent of PI in abc and predictive DB controller.

a) *Equivalent of PI in abc frame*: The grid current harmonic spectrum using the implementation of (4) is depicted in Fig. 11(a). A slightly lower magnitude for all harmonic orders can be observed compared to the dq implementation of the same controller. This is also proved by the THD value, which in this situation is 1.72%.

b) *DB controller*: Fig. 11(b) illustrates the harmonic spectrum of the grid current in the case when DB controller is used for current regulation. The THD in this situation measured by the power meter is 2.4%.

B. Transient Operation Conditions

The tests for transient operation conditions are divided into two types. First, a step in the current reference is generated such

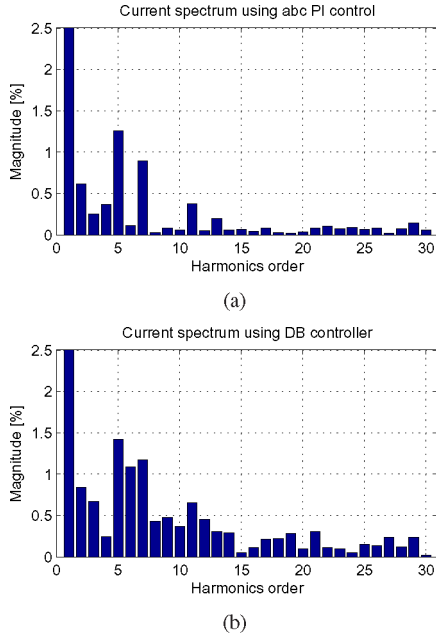


Fig. 11. Harmonic spectrum of the grid current in the case of (a) equivalent of PI used in *abc* frame and (b) DB control.

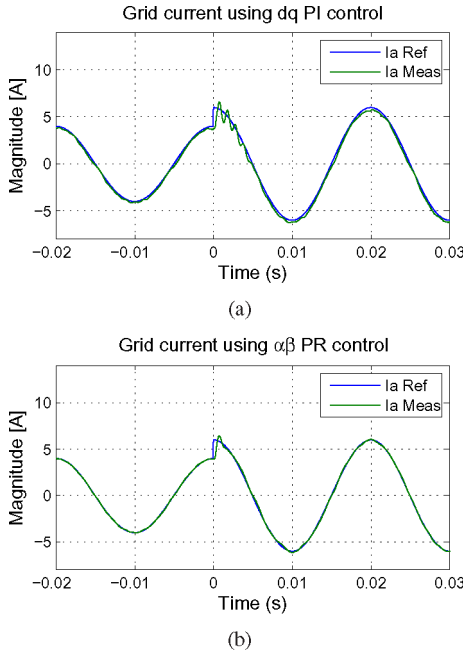


Fig. 12. Dynamics of the controllers in the case of 2 A current reference step. (a) PI controller implemented in *dq* frame. (b) PR controller in stationary frame.

that the output power of the converter increases from 2 up to 3 kW. The dynamics of the controllers are pursued during this experiment. Second, the behavior of the current controller in the case of single-phase grid fault is examined.

1) *Step in Reference Current*: Fig. 12(a) depicts the response of the PI controller implemented in *dq* synchronous frame when a step in the current reference is issued. As it might be observed, the controller has very high dynamics, following closely the imposed reference. The responses of the other controllers are

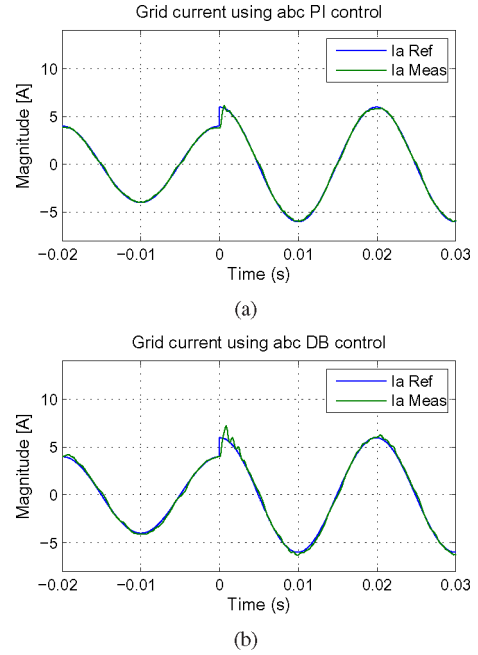


Fig. 13. Dynamics of the controllers in the case of 2 A current reference step. (a) Equivalent of PI in *abc* frame. (b) DB controller in *abc* frame.

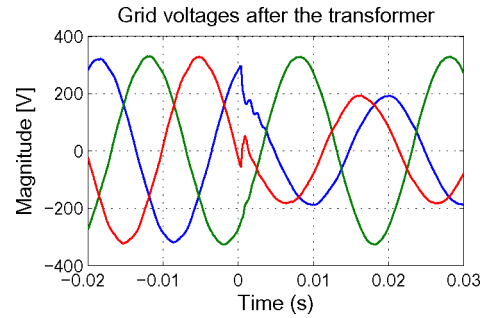


Fig. 14. Grid voltages after the Δy transformer in the case of single-phase fault at the point of common coupling.

shown in Figs. 12(b) and 13(b). Note that all controllers have a good and fast transient response in this situation.

2) *Single-Phase Grid Fault*: It has been shown in [12] that in the case of single-phase fault in the grid, the voltages after the Δy transformer (at the converter terminals) behave in a manner as illustrated in Fig. 14. The grid simulator has been programmed to produce zero voltage on one phase at the time instant 0 s. As a consequence, amplitude drop and phase jump in two of the phases are registered, as illustrated in Fig. 14. Under such unbalanced grid conditions, the synchronization algorithm has an important role in the control. A phase-locked loop (PLL) system, which is able to extract the positive sequence of the grid voltages, has been used [35], and hence, the phase angle provided by the algorithm during the fault is synchronized to the positive sequence component of the grid voltages. In this situation, the current references remain sinusoidal and balanced, as described in [36].

a) *The dq control structure*: Looking at the controlled current using *dq* control structure [Fig. 15(a)], a small disturbance

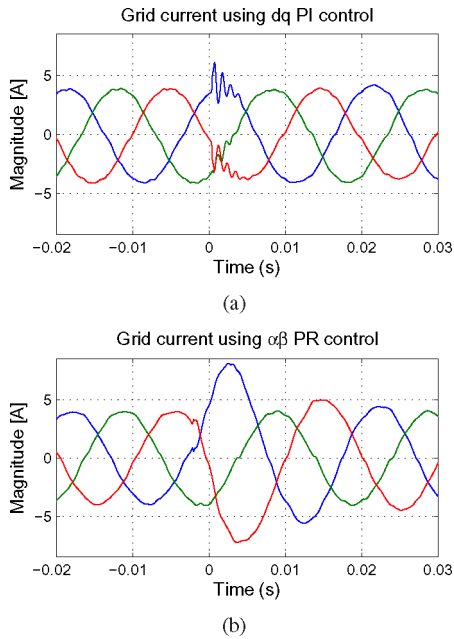


Fig. 15. Response of the controller in the case of single-phase fault. (a) PI controller implemented in dq frame. (b) PR controller in stationary frame.

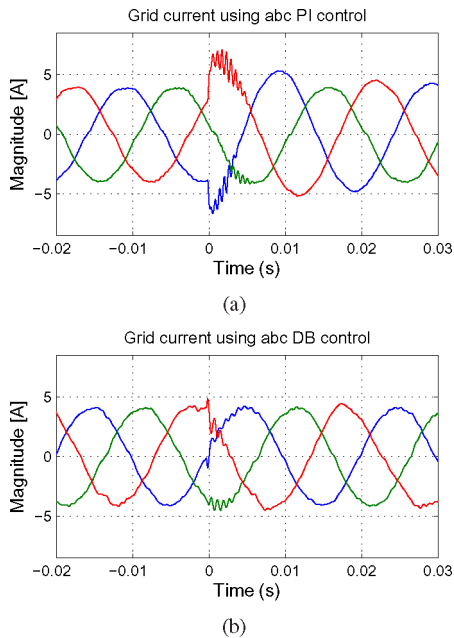


Fig. 16. Response of the controller in the case of single-phase fault. (a) Equivalent of PI in abc frame. (b) DB controller in abc frame.

can be observed in the current waveform when the fault occurs, but this is fast regulated according to the imposed reference. The grid voltage feedforward terms used in this control structure play an important role here, enhancing the dynamics of the controller in the situation of grid voltage variations.

b) Stationary frame control structure: The behavior of the PR controller implemented in stationary frame is depicted in Fig. 15(b). As it might be noted, in this case, the controller has a larger overshoot in its response when the grid fault takes place. Anyway, this is not too large to trip out the current protection

of the system and the current is fast controlled according to its reference within one fundamental period. Note that in this case, no grid voltage feedforward terms are used in the controller.

c) Equivalent of PI in abc frame: A similar behavior is registered by the equivalent of PI controller implemented in natural reference frame. Anyway, the overshoot in this case is not as large as in the case of the PR controller and the current is also fast regulated soon after the fault.

d) DB control: The response of the DB controller in the case of grid fault is shown in Fig. 16(b). Compared to all previous behaviors, the DB controller has the highest robustness in a situation of a grid fault. A small transient in the controlled current waveform can be observed when the fault occurs, but the current value does not exhibit any overshoot, following closely the imposed reference.

VIII. CONCLUSION

This paper has given a description of some possible control structures for DPGSs connected to utility network. The traditional synchronous reference frame structure were well as stationary reference frame and natural reference frame structures were addressed in this paper. The control structures were illustrated and their major characteristics were described.

Additionally, a few types of controllers have been discussed, namely PI controllers implemented in dq frame, the resonant controller, PI controller implemented in abc frame, and finally, the DB predictive controller. Their design for grid-connected applications was described and an evaluation of these controllers in terms of harmonic distortion when running in steady-state conditions was done. Moreover, the performance of the controllers in situation of reference current step-up and a single-phase fault situation has been investigated. All controllers prove to have a satisfactory behavior in all situations but a DB controller proves to be superior to the others especially during grid fault.

REFERENCES

- [1] EWEA. (2005, Oct.). Documentation [Online]. Available: www.ewea.org/documents
- [2] IEA-PVPS. (2005, Oct.). Cumulative installed PV power [Online]. Available: www.iea-pvps.org
- [3] F. Blaabjerg, Z. Chen, and S. Kjaer, "Power electronics as efficient interface in dispersed power generation systems," *IEEE Trans. Power Electron.*, vol. 19, no. 5, pp. 1184–1194, Sep. 2004.
- [4] E.ON Netz. (2006). Grid code—High and extra high voltage. E.ON Netz GmbH, Tech. Rep. [Online]. Available: <http://www.eon-netz.com/Ressources/downloads/ENENARHS2006eng.pdf>
- [5] Eltra and Elkraft. (2004). Wind turbines connected to grids with voltage below 100 kV [Online]. Available: <http://www.eltra.dk>
- [6] J. Carrasco, L. Franquelo, J. Bialasiewicz, E. Galvan, R. PortilloGuisado, M. Prats, J. Leon, and N. Moreno-Alfonso, "Power-electronic systems for the grid integration of renewable energy sources: A survey," *IEEE Trans. Ind. Electron.*, vol. 53, no. 4, pp. 1002–1016, Jun. 2006.
- [7] *IEEE Standard for Interconnecting Distributed Resources With Electric Power Systems*, IEEE Standard 15471, 2005.
- [8] *Photovoltaic (PV) Systems, Characteristics of the Utility Interface*, IEC Standard 61727, Ed. 2.0, Standard, 2004.
- [9] *Wind Turbines, Measurement and Assessment of Power Quality Characteristics of Grid Connected Wind Turbines—Part 21*, IEC Standard 61400-21, Ed. 2.0, Standard, 2008.
- [10] *Electromagnetic Compatibility (EMC), Testing and Measurement Techniques—General Guide on Harmonics and Interharmonics Measurements and Instrumentation, for Power Supply Systems and Equipment*

- Connected Thereto—Part 4-7, IEC Standard 61400-4-7, Ed. 2.0, Standard, 2002.
- [11] *Electromagnetic Compatibility (EMC), Limits—Assessment of Emission Limits for the Connection of Distorting Installations to MV, HV and EHV Power Systems—Part 3-6*, IEC/TR Standard 61000-3-6, Ed. 2.0, Standard, 2008, 2009.
- [12] M. H. J. Bollen, *Understanding Power Quality Problems: Voltage Sags and Interruptions*. Piscataway, NJ: IEEE Press, 2002.
- [13] S. Fukuda and T. Yoda, “A novel current-tracking method for active filters based on a sinusoidal internal model,” *IEEE Trans. Ind. Electron.*, vol. 37, no. 3, pp. 888–895, May/June 2001.
- [14] Y. Sato, T. Ishizuka, K. Nezu, and T. Kataoka, “A new control strategy for voltage-type PWM rectifiers to realize zero steady-state control error in input current,” *IEEE Trans. Ind. Appl.*, vol. 34, no. 3, pp. 480–486, May/June 1998.
- [15] X. Yuan, W. Merk, H. Stemmler, and J. Allmeling, “Stationary-frame generalized integrators for current control of active power filters with zero steady-state error for current harmonics of concern under unbalanced and distorted operating conditions,” *IEEE Trans. Ind. Appl.*, vol. 38, no. 2, pp. 523–532, Mar./Apr. 2002.
- [16] R. Teodorescu, F. Blaabjerg, U. Borup, and M. Liserre, “A new control structure for grid-connected LCL PV inverters with zero steady-state error and selective harmonic compensation,” in *Proc. IEEE APEC 2004*, vol. 1, pp. 580–586.
- [17] R. Teodorescu and F. Blaabjerg, “Proportional-resonant controllers. A new breed of controllers suitable for grid-connected voltage-source converters,” in *Proc. OPTIM 2004*, vol. 3, pp. 9–14.
- [18] A. V. Timbus, M. Ciobotaru, R. Teodorescu, and F. Blaabjerg, “Adaptive resonant controller for grid-connected converters in distributed power generation systems,” in *Proc. IEEE APEC 2006*, pp. 1601–1606.
- [19] M. Kazmierkowski and M. Dzieniakowski, “Review of current regulation methods for VS-PWM inverters,” in *Proc. ISIE 1993*, pp. 448–456.
- [20] S. Buso, L. Malesani, and P. Mattavelli, “Comparison of current control techniques for active filter applications,” *IEEE Trans. Ind. Electron.*, vol. 45, no. 5, pp. 722–729, Oct. 1998.
- [21] D. N. Zmood, D. G. Holmes, and G. H. Bode, “Frequency-domain analysis of three-phase linear current regulators,” *IEEE Trans. Ind. Appl.*, vol. 37, no. 2, pp. 601–610, Mar./Apr. 2001.
- [22] E. Twining and D. G. Holmes, “Grid current regulation of a three-phase voltage source inverter with an LCL input filter,” *IEEE Trans. Power Electron.*, vol. 18, no. 3, pp. 888–895, May 2003.
- [23] S. Buso, S. Fasolo, and P. Mattavelli, “Uninterruptible power supply multi-loop control employing digital predictive voltage and current regulators,” in *Proc. IEEE APEC 2001*, vol. 2, pp. 907–913.
- [24] Y. Ito and S. Kawauchi, “Microprocessor based robust digital control for UPS with three-phase PWM inverter,” *IEEE Trans. Power Electron.*, vol. 10, no. 2, pp. 196–204, Mar. 1995.
- [25] T. Kawabata, T. Miyashita, and Y. Yamamoto, “Dead beat control of three phase PWM inverter,” *IEEE Trans. Power Electron.*, vol. 5, no. 1, pp. 21–28, Jan. 1990.
- [26] J. Kolar, H. Ertl, and F. Zach, “Analysis of on- and off-line optimized predictive current controllers for PWM converter systems,” *IEEE Trans. Power Electron.*, vol. 6, no. 3, pp. 451–462, Jul. 1991.
- [27] P. Mattavelli, G. Spiazzi, and P. Tenti, “Predictive digital control of power factor preregulators with input voltage estimation using disturbance observers,” *IEEE Trans. Power Electron.*, vol. 20, no. 1, pp. 140–147, Jan. 2005.
- [28] S.-G. Jeong and M.-H. Woo, “DSP-based active power filter with predictive current control,” *IEEE Trans. Ind. Electron.*, vol. 44, no. 3, pp. 329–336, Jun. 1997.
- [29] R. Wu, S. Dewan, and G. Slemon, “Analysis of a PWM AC to DC voltage source converter under the predicted current control with a fixed switching frequency,” *IEEE Trans. Ind. Appl.*, vol. 27, no. 4, pp. 756–764, Jul./Aug. 1991.
- [30] K. Macken, K. Vanthournout, J. Van den Keybus, G. Deconinck, and R. Belmans, “Distributed control of renewable generation units with integrated active filter,” *IEEE Trans. Power Electron.*, vol. 19, no. 5, pp. 1353–1360, Sep. 2004.
- [31] A. Dell’Aquila, A. Lecci, and M. Liserre, “Microcontroller-based fuzzy logic active filter for selective harmonic compensation,” in *Proc. IAS 2003*, Oct. 12–16, vol. 1, pp. 285–292.
- [32] L. Malesani, P. Mattavelli, and S. Buso, “Robust dead-beat current control for PWM rectifiers and active filters,” *IEEE Trans. Ind. Appl.*, vol. 35, no. 3, pp. 613–620, May/June 1999.
- [33] G. Bode, P. C. Loh, M. Newman, and D. Holmes, “An improved robust predictive current regulation algorithm,” *IEEE Trans. Ind. Appl.*, vol. 41, no. 6, pp. 1720–1733, Nov./Dec. 2005.
- [34] Y. A.-R. I. Mohamed and E. F. El-Saadany, “An improved deadbeat current control scheme with a novel adaptive self-tuning load model for a three-phase PWM voltage-source inverter,” *IEEE Trans. Ind. Electron.*, vol. 54, no. 2, pp. 747–759, Apr. 2007.
- [35] A. V. Timbus, M. Liserre, F. Blaabjerg, R. Teodorescu, and P. Rodriguez, “PLL algorithm for power generation systems robust to grid faults,” in *Proc. IEEE PESC 2006*, pp. 1360–1366.
- [36] P. Rodriguez, A. Timbus, R. Teodorescu, M. Liserre, and F. Blaabjerg, “Flexible active power control of distributed power generation systems during grid faults,” *IEEE Trans. Ind. Electron.*, vol. 54, pp. 2583–2592, 2007.



Adrian Timbus (S’04–M’08) received the Diploma in engineering and the Master’s degree from the Technical University of Cluj, Cluj-Napoca, Romania, in 2000 and 2001, respectively, and the M.Sc.E.E. and Ph.D. degrees from Aalborg University, Aalborg, Denmark, in 2003 and 2007, respectively.

He is currently with Corporate Research, ABB Switzerland Ltd., Switzerland. His current research interests include integration of distributed generation, and management and control of active distribution networks.

Dr. Timbus is a member of the IEEE Power Electronics Society, the IEEE Industrial Electronics Society, and the IEEE Power Engineering Society.



Marco Liserre (S’00–M’02–SM’07) received the M.Sc. and Ph.D. degrees in electrical engineering from the Politecnico di Bari, Bari, Italy, in 1998 and 2002, respectively.

He is currently an Assistant Professor at the Politecnico di Bari. His current research interests include power converters and drives, namely the control of converters, power quality, and distributed generation. He has authored or coauthored about 114 technical papers, 26 of them published or to be published in peer-reviewed international journals. He is

the coauthor of three chapters of the book *Electromagnetic Compatibility in Power Systems* (Elsevier, 2006).

Dr. Liserre is a member of the IEEE Industry Applications Society, the IEEE Industrial Electronics Society, and the IEEE Power Electronics Society. He was an AdCom Member of the IEEE Industrial Electronics Society during 2003–2004, the Chair for Student Activities during 2002–2004, the Chair for Region 8 Membership Activities since 2004, and a Newsletter Editor since 2005. He is an Associate Editor of the IEEE TRANSACTION ON INDUSTRIAL ELECTRONICS. He is the Editor-in-Chief of the new IEEE INDUSTRIAL ELECTRONICS MAGAZINE.



Remus Teodorescu (S’94–A’97–M’99–SM’02) received the Dipl.Ing. degree in electrical engineering from the Polytechnic University of Bucharest, Bucharest, Romania, in 1989, and the Ph.D. degree from the University of Galati, Galati, Romania, in 1994.

From 1989 to 1990, he was with the Iron and Steel Plant, Galati. He was an Assistant Professor in the Department of Electrical Engineering, Galati University. In 1998, he joined the Power Electronics Section, Institute of Energy Technology, Aalborg

University, Aalborg, Denmark, where he is currently a full Professor. His current research interests include power converters for renewable energy systems (photovoltaic (PV), wind turbines) and electrical drives. He has authored or coauthored more than 100 technical papers, 12 of them published in journals. He is the coauthor of two books, and holds five patents.

Dr. Teodorescu is an Associate Editor for the IEEE TRANSACTIONS ON POWER ELECTRONICS LETTERS and the Chair of the IEEE Danish Industry Applications Society (IAS)/Industrial Electronics Society (IES)/Power Electronics Society (PELS) Chapter. He received the Technical Committee Prize Paper Awards at IEEE-IAS98 and the OPTIM-ABB Prize Paper Award at OPTIM 2002.



Pedro Rodriguez (S'01–A'03–M'04) received the B.S. degree in electrical engineering from the University of Granada, Granada, Spain, in 1989, and the M.S. and Ph.D. degrees in electrical engineering from the Technical University of Catalonia (UPC), Catalonia, Spain, in 1994 and 2004, respectively.

In 1990, he joined the faculty of UPC as an Assistant Professor, where he became an Associate Professor in 1993. During 2005–2006, he was a Researcher in the Center for Power Electronics Systems (CPES), Virginia Polytechnic Institute and State University, Blacksburg, and in the Institute of Energy Technology (IET), Aalborg University, Aalborg, Denmark. He is currently the Head of the Electrical Engineering Research Group, UPC's Terrassa Campus. His current research interests include power conditioning, integration of distributed energy systems, and control of power converters.



Frede Blaabjerg (S'86–M'88–SM'97–F'03) received the M.Sc.E.E. degree from Aalborg University, Aalborg, Denmark, in 1987, and the Ph.D. degree from the Institute of Energy Technology, Aalborg University, in 1995.

From 1987 to 1988, he was with ABB-Scandia, Randers. He is currently with Aalborg University, where he became an Assistant Professor in 1992, an Associate Professor in 1996, a Full Professor of power electronics and drives in 1998, and the Dean of Faculty of Engineering and Science in 2006. He is an Associate Editor of the *Journal of Power Electronics* and Danish journal *Elteknik*. His current research interests include power electronics, static power converters, ac drives, switched reluctance drives, modeling and characterization of power semiconductor devices and simulation, wind turbines, and green power inverters. He has authored or coauthored more than 300 papers including the book *Control in Power Electronics* (Academic Press, 2002).

Dr. Blaabjerg has held a number of Chairman positions in research policy and research funding bodies in Denmark. He is an Associate Editor of the IEEE TRANSACTIONS ON INDUSTRY APPLICATIONS and the IEEE TRANSACTIONS ON POWER ELECTRONICS. In 2006, he became the Editor-in-Chief of the IEEE TRANSACTIONS ON POWER ELECTRONICS. He received the 1995 Angelos Award for his contribution in modulation technique and control of electric drives, and the Annual Teacher Prize at Aalborg University in 1995. In 1998, he received the Outstanding Young Power Electronics Engineer Award from the IEEE Power Electronics Society. He had received five IEEE Prize Paper Awards during the last six years. He received the C.Y. O'Connor Fellowship 2002 from Perth, Australia, the Statoil-Prize in 2003 for his contributions in power electronics, and the Grundfos Prize in 2004 for his contributions in power electronics and drives.